

# Stratified exchange flows of two Bingham fluids in an inclined slot

I.A. Frigaard

*Schlumberger Dowell, 26 rue de la Cavée, 92140 Clamart, France*

Received 27 October 1997; received in revised form 18 December 1997

---

## Abstract

Buoyancy driven flows of two Bingham fluids in an inclined slot are considered, providing a simplified model for the plug cementing process. The flows studied are near-uniaxial and stratified, with the heavy fluid moving down the incline, displacing the lighter fluid upwards. There is no net axial volume flux. Four qualitatively different types of velocity solution profiles,  $u$ , are shown to exist, three of which are non-trivial. The regions of existence of each flow type can be described parametrically in terms of the two dimensionless fluid yield stresses,  $(\tau_{c,Y}, \tau_{m,Y})$ , and the dimensionless interface height in the slot,  $h$ . The boundary of the region in the  $(\tau_{c,Y}, \tau_{m,Y})$  plane, outside of which only the trivial solution  $u = 0$  exists, is determined exactly and a simple analytic expression is given. Within this region, perturbation methods are used to produce asymptotic approximations to the flow rates and interface velocities for values of  $h$  such that  $u \neq 0$ . The perturbation solutions are used to study axial propagation of the interface height profile  $h(x, t)$  along the slot. © 1998 Elsevier Science B.V. All rights reserved.

---

## 1. Introduction

Plug cementing is a relatively common operation carried out both when drilling and abandoning oil wells [1]. When setting a cement plug above the bottom of the wellbore, one places a heavy cement slurry, (*c.*  $1900 \text{ kg m}^{-3}$ ), above a lighter fluid (e.g. *drilling mud* or *viscous pill*: density  $1200\text{--}1700 \text{ kg m}^{-3}$ ). The wellbore is typically inclined from vertical, is approximately cylindrical of diameter  $\leq 0.3 \text{ m}$ , and has length of the order  $\sim 10^3 \text{ m}$ . Cement plug lengths are typically  $\sim 100 \text{ m}$  and the cement is placed so as to completely fill the wellbore cross-section.

It is necessary for the cement to remain static for a period of hours while it sets. This situation is mechanically unstable and, if the fluids were Newtonian, the cement would fall through the lighter fluids and end up at the bottom of the wellbore. This does not typically happen. Both drilling muds and cement slurries have complex rheologies. For modelling fluid motion, these fluids are easiest described by viscoplastic constitutive models (e.g. Bingham, Herschel–Bulkley,

Casson). Such a description is not completely accurate since thixotropy and viscoelastic effects can also be important. However, plastic viscosity and yield point figures are regularly used to characterise these oilfield fluids, making the Bingham model attractive.

The setting of cement plugs has received much attention in the technical literature over the years, e.g. [2–6]. Although mechanical supports are sometimes utilised [5], this is not standard industry practice. The fundamental problem remains, of determining the fluid properties required to stably maintain a heavy cement plug over a lighter fluid. In [2] a fully axisymmetric buoyant flow is considered, but this case is only likely to occur if the wellbore is perfectly vertical and the initial interface is axisymmetric. In experiments using oilfield fluids in a closed ended pipe [4], the heavy cement slumps towards the low side of the pipe and slides in an approximately axial direction down the pipe, displacing mud upwards. The initial interface between the two fluids becomes axially elongated during this motion. If the fluids used are somehow *close* to being stable (i.e. static), the motion is slow, laminar and the interface between fluids remains well-defined.

It is the above type of flow that is studied in this paper. Two Bingham fluids of different densities and rheologies are taken to represent the mud and cement. The only driving force for the flow is that of buoyancy, resulting from the density difference between the fluids. Of primary interest here is the interaction between viscoplastic and buoyancy forces. An additional complication in a pipe geometry is the interface configuration which, although it develops axially into a *long-thin* geometry, is otherwise arbitrary. To remove this complication, a simple slot geometry is considered and the flow is assumed *a priori* to be two-dimensional. This geometrical simplification allows the application of classical applied mathematical methods, leading to simple physical insights.

There are numerous studies of laminar flows of a single Bingham fluid in simple geometries (e.g. [7–9]). Perhaps the most relevant of recent studies is [10], which considers the slow spreading of a Bingham fluid on an inclined plane. Once the geometry becomes even slightly complex, the solutions to Bingham fluid flow problems can exhibit a rich structure and flow features are found that are not found with Newtonian fluids, (e.g. see [11,12] on axial flows through an eccentric annulus). Hence, what appears here as a simple flow must be treated with some respect.

In outline the paper is as follows. Section 2 following, introduces the physical models, derives a suitable mathematical approximation and considers physical constraints on the solution. In Section 3, the momentum balance is uncoupled and analysed, in order to determine different possible solution types in terms of the axial velocity  $u$ . Reformulation of the problem as a constrained optimisation problem allows the derivation of sufficient conditions to ensure  $u=0$ . Perturbation methods are used to show that these conditions are also necessary and to derive asymptotic approximations for flow rates and interface velocities when  $u \neq 0$ . Interface propagation is considered in Section 4 and order of magnitude estimates are given for the propagation speed. The paper concludes with a brief discussion, Section 5.

The more complex (and physically realistic) problem of uniaxial flows of two Bingham fluids in a pipe geometry with an arbitrary cross-sectional fluid–fluid interface has also been addressed [13]. The approach taken is akin to that in [14–16].

## 2. Physical model

Consider a two-dimensional slot geometry and coordinates as shown in Fig. 1. The slot axis is inclined at an angle  $\beta$  to the vertical direction of gravity and is assumed to contain a cement slurry of density  $\hat{\rho}_c$  and a drilling mud of density  $\hat{\rho}_m$ . It is assumed that  $\hat{\rho}_c > \hat{\rho}_m$ . Suppose that the heavier fluid (cement) has initially been placed above ( $\hat{x}$  large and positive) and lighter fluid (mud). Under the action of gravity, the cement slides down the lower wall of the slot displacing the mud upwards, against the upper wall of the slot. As this motion continues, the interface elongates into the situation shown in Fig. 1. The fluids are assumed miscible, but not mixed. There are no interfacial forces, i.e. surface tension, and there is no mass transfer at the interfaces between mud and cement, e.g. no chemical reactions between the fluids. The fluid–fluid interface between cement and mud is denoted

$$\hat{y} = \hat{h}(\hat{x}, \hat{t}). \quad (2.1)$$

The slot width is denoted  $\hat{D}$  and the slot length considered is denoted  $\hat{L}$ . It is assumed that

$$\delta \equiv \frac{\hat{D}}{\hat{L}} \ll 1. \quad (2.2)$$

The pressure and velocity are denoted  $\hat{p}(\hat{x}, \hat{y}, \hat{t})$  and  $\hat{u}(\hat{x}, \hat{y}, \hat{t}) = (\hat{u}, \hat{v})$ , respectively. The stress and deviatoric stress tensors are denoted  $\hat{\sigma}_{k,ij}$  and  $\hat{\tau}_{k,ij}$ , respectively. Since the flow is assumed two-dimensional, the indices  $i, j$  range over only 1, 2, with 1 denoting the  $\hat{x}$  direction, as is conventional. Dimensional quantities are distinguished with a *hat* symbol,  $\hat{\cdot}$ , and the index  $k$  is used throughout to denote the fluid present, i.e.  $k = c$  for cement,  $k = m$  for mud.

The equations of motion, valid within each fluid region, are

$$\hat{\rho}_k \frac{d\hat{u}_i}{d\hat{t}} = \frac{\partial}{\partial \hat{x}_j} \hat{\sigma}_{k,ij} + \hat{G}_{k,i}, \quad k = c, m, \quad i = 1, 2, \quad (2.3)$$

$$0 = \frac{\partial \hat{u}}{\partial \hat{x}} + \frac{\partial \hat{v}}{\partial \hat{y}}, \quad (2.4)$$

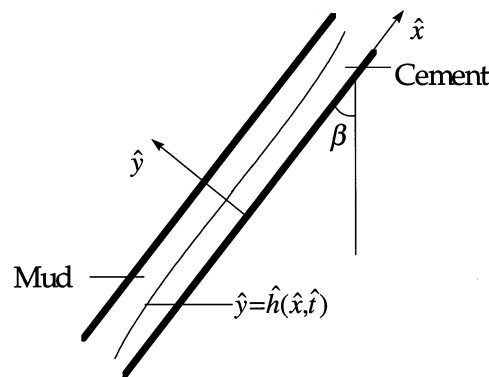


Fig. 1. Schematic of slot geometry and coordinates.

where the gravitational body force  $\hat{G}_k$  is defined by

$$\hat{G}_k = (-\hat{\rho}_k \hat{g} \cos \beta, -\hat{\rho}_k \hat{g} \sin \beta), \quad (2.5)$$

and

$$\frac{d}{dt} \equiv \frac{\partial}{\partial t} + \hat{u} \frac{\partial}{\partial \hat{x}} + \hat{v} \frac{\partial}{\partial \hat{y}}.$$

At the walls of the slot the no-slip condition is satisfied:

$$\hat{u} = 0. \quad (2.6)$$

The unit normal to the fluid–fluid interface is denoted  $n$ :

$$n = \frac{1}{\left[1 + \left(\frac{\partial \hat{h}}{\partial \hat{x}}\right)^2\right]^{1/2}} \left(-\frac{\partial \hat{h}}{\partial \hat{x}}, 1\right) \quad (2.7)$$

and the interface velocity is denoted  $\hat{u}_{\text{int}}$ . Velocity and stress vectors are continuous across the interface, i.e.

$$\hat{u} = \hat{u}_{\text{int}}, \quad (2.8)$$

$$(-\hat{p}_c \delta_{ij} + \hat{\tau}_{c,ij}) n_j = (-\hat{p}_m \delta_{ij} + \hat{\tau}_{m,ij}) n_j, \quad (2.9)$$

where  $\hat{p}_k$  has been used to denote the limiting value of the pressure as the interface is approached from the side of fluid  $k$ . The interface itself is a material surface, advected by the flow. Thus,  $\hat{h}$  satisfies

$$\frac{\partial \hat{h}}{\partial t} + \hat{u}(\hat{x}, \hat{h}, \hat{t}) \frac{\partial \hat{h}}{\partial \hat{x}} = \hat{v}(\hat{x}, \hat{h}, \hat{t}). \quad (2.10)$$

The *area flow rates* along the slot, in the cement layer and in the mud layer are denoted by  $\hat{Q}$ ,  $\hat{Q}_c$  and  $\hat{Q}_m$ , respectively. These quantities are defined by

$$\hat{Q}_c = \int_0^{\hat{h}} \hat{u} \, d\hat{y}, \quad (2.11)$$

$$\hat{Q}_m = \int_{\hat{h}}^{\hat{D}} \hat{u} \, d\hat{y}, \quad (2.12)$$

$$\hat{Q} = \hat{Q}_c + \hat{Q}_m. \quad (2.13)$$

Combining Eq. (2.4) with Eq. (2.10) leads to

$$\frac{\partial \hat{h}}{\partial t} + \frac{\partial}{\partial \hat{x}} \hat{Q}_c = 0. \quad (2.14)$$

### 2.0.1. Exchange flow constraint

The bottom of the slot, ( $-\hat{x}$  large), far away from the region of interest, denotes the bottom of the wellbore. This is typically sealed and the fluids are incompressible. Thus, there is an exchange of fluids in the axial direction, which is what is meant by the term *exchange flow*, i.e. the constraint

$$\hat{Q}(\hat{u}) = 0, \quad (2.15)$$

is satisfied; there is no net axial flow.

### 2.0.2. Constitutive laws

The fluid rheologies assumed are those of incompressible Bingham fluids. Rate of strain and deviatoric stress second invariants,  $\hat{\gamma}(\hat{u})$  and  $\hat{\tau}_k(\hat{u})$  respectively, are defined by

$$\hat{\gamma}(\hat{u}) = \left[ \frac{1}{2} \sum_{i,j=1}^2 [\hat{\gamma}_{ij}(\hat{u})]^2 \right]^{1/2}, \quad (2.16)$$

$$\hat{\tau}_k(\hat{u}) = \left[ \frac{1}{2} \sum_{i,j=1}^2 [\tau_{k,ij}(\hat{u})]^2 \right]^{1/2}, \quad (2.17)$$

where

$$\hat{\gamma}_{ij}(\hat{u}) = \frac{\partial \hat{u}_i}{\partial \hat{x}_j} + \frac{\partial \hat{u}_j}{\partial \hat{x}_i}. \quad (2.18)$$

Constitutive laws for the Bingham fluids are

$$\hat{\gamma}(\hat{u}) = 0 \Leftrightarrow \hat{\tau}_k(\hat{u}) \leq \hat{\tau}_{k,Y}, \quad \hat{x} \in V_k, \quad (2.19)$$

$$\hat{\tau}_{k,ij}(\hat{u}) = \left[ \hat{\mu}_k + \frac{\hat{\tau}_{k,Y}}{\hat{\gamma}(\hat{u})} \right] \hat{\gamma}_{ij}(\hat{u}) \Leftrightarrow \hat{\tau}_k(\hat{u}) > \hat{\tau}_{k,Y}, \quad \hat{x} \in V_k. \quad (2.20)$$

The constants  $\hat{\mu}_k$  and  $\hat{\tau}_{k,Y}$  are the plastic viscosity and yield stress, respectively, for each fluid:  $k = c, m$ . These parameters are assumed to be strictly positive.

## 2.1. Scaled equations

It is assumed that the flow is near uniaxial, in the following sense:

(i) The fluid–fluid interface is quasi-parallel to the slot axis:

$$\left| \frac{\partial \hat{h}}{\partial \hat{x}} \right| = O(\delta). \quad (2.21)$$

(ii) The streamlines are quasi-parallel to the slot axis, such that if  $\hat{u}_*$  denotes an axial velocity scale then  $\delta \hat{u}_*$  denotes a non-axial velocity scale, i.e.

$$\delta \hat{u} \sim \hat{v}. \quad (2.22)$$

With the assumptions that have already been made, the flow described is a stratified shear flow, driven by buoyancy, i.e. by the density difference between the fluids. Since both fluids have Bingham rheologies, the two fluid layers can be expected to consist of both yielded and

unyielded regions of flow. In a yielded region of the flow, the constitutive equations (Eq. (2.20)) fully determine the deviatoric stress and because of Eq. (2.22) the following scaling will be valid:

$$\delta \hat{\tau}_{k,12} = \delta \hat{\tau}_{k,21} \sim \hat{\tau}_{k,11} \sim \hat{\tau}_{k,22}. \quad (2.23)$$

Both the scalings Eqs. (2.22) and (2.23) will be valid up to the boundary of an unyielded region, by continuity. Within an unyielded region, since  $\hat{\gamma}(\hat{u}) = 0$ , the velocity scaling Eq. (2.22) must remain valid. This might not be true of the deviatoric stress scaling Eq. (2.23); however, the validity of Eq. (2.23) in any unyielded region will be assumed, (see Ref. [13]).

Dimensionless spatial coordinates and velocities are defined as follows:

$$\hat{x} = x\hat{L}, \quad (2.24)$$

$$\hat{y} = y\hat{D}, \quad (2.25)$$

$$\hat{u} = u\hat{u}_*, \quad (2.26)$$

$$\hat{v} = v\delta\hat{u}_*. \quad (2.27)$$

The timescale  $\hat{t}_*$  and dimensionless time  $t$  are defined by

$$\hat{t}_* \equiv \frac{\hat{L}}{\hat{u}_*}; \quad \hat{t} = \hat{t}_*t. \quad (2.28)$$

Interface height and the area flow rates are scaled straightforwardly:

$$\hat{h} = \hat{D}h, \quad (2.29)$$

$$\hat{Q}_k = \hat{u}_*\hat{D}Q_k, \quad k = \cdot, c, m. \quad (2.30)$$

The mean density and the density difference are defined by

$$\hat{\rho} = \frac{1}{2}[\hat{\rho}_c + \hat{\rho}_m], \quad (2.31)$$

$$\Delta\hat{\rho} = \hat{\rho}_c - \hat{\rho}_m, \quad (2.32)$$

and the following definitions are made for algebraic convenience:

$$\phi_c = \frac{\hat{\rho}_c}{\hat{\rho}}, \quad \phi_m = \frac{\hat{\rho}_m}{\hat{\rho}}, \quad \phi = \frac{\Delta\hat{\rho}}{\hat{\rho}}. \quad (2.33)$$

Note that  $\phi_c + \phi_m = 2$  and  $\phi_c - \phi_m = \phi$ . A dimensionless pressure is defined by

$$p(x, y, t) = \frac{\hat{p}(\hat{x}, \hat{y}, \hat{t}) - \hat{p}_0}{\hat{\rho}\hat{g}\hat{L}\cos\beta} \quad (2.34)$$

where  $\hat{p}_0$  denotes a constant reference pressure, say at the coordinate origin. It is assumed that the slot is far from horizontal, in the sense that

$$0 \ll \cos\beta \leq 1. \quad (2.35)$$

For the flow to remain non-inertial there must be a balance between the leading order deviatoric stress gradients (the visco-plastic forces) and the buoyancy gradient acting in the axial direction:

$$\frac{\hat{\tau}_k}{\hat{D}} \sim \Delta \hat{\rho} \hat{g} \cos \beta. \quad (2.36)$$

Combining this with Eq. (2.23) gives

$$\tau_{k,12} = \tau_{k,21} = \frac{\hat{\tau}_{k,12}}{\Delta \hat{\rho} \hat{g} \hat{D} \cos \beta}, \quad (2.37)$$

$$\tau_{k,11} = \frac{\hat{\tau}_{k,11}}{\Delta \hat{\rho} \hat{g} \hat{L} \cos \beta}, \quad (2.38)$$

$$\tau_{k,22} = \frac{\hat{\tau}_{k,22}}{\Delta \hat{\rho} \hat{g} \hat{L} \cos \beta}. \quad (2.39)$$

Following the above scalings, the dimensionless field equations are

$$\frac{\phi_k \hat{u}_*^2}{\phi \hat{g} \hat{L} \cos \beta} \frac{du}{dt} = -\frac{1}{\phi} \left[ \frac{\partial p}{\partial x} + \phi_k \right] + \frac{\partial \tau_{k,xy}}{\partial y} + \delta^2 \frac{\partial \tau_{k,xx}}{\partial x}, \quad (2.40)$$

$$\delta^2 \frac{\phi_k \hat{u}_*^2}{\phi \hat{g} \hat{L} \cos \beta} \frac{dv}{dt} = -\frac{1}{\phi} \left[ \frac{\partial p}{\partial y} + \phi_k \delta \tan \beta \right] + \delta^2 \left[ \frac{\partial \tau_{k,xy}}{\partial x} + \frac{\partial \tau_{k,yy}}{\partial y} \right], \quad (2.41)$$

$$\frac{\partial u}{\partial x} + \frac{\partial v}{\partial y} = 0, \quad (2.42)$$

$$\frac{\partial h}{\partial t} + \frac{\partial Q_c}{\partial x} = 0. \quad (2.43)$$

Boundary conditions at the slot wall are

$$u = 0, \quad (2.44)$$

and (to leading order) at the interface:

$$\tilde{u} = \tilde{u}_{\text{int}}, \quad (2.45)$$

$$\tau_{c,xy} = \tau_{m,xy}, \quad (2.46)$$

$$\hat{p}_m = \hat{p}_c. \quad (2.47)$$

## 2.2. Uniaxial flow equations

Making the assumption that

$$\hat{u}_*^2 \sim \frac{\Delta \hat{\rho} \hat{g} \hat{D} \cos \beta}{\hat{\rho}_k}, \quad (2.48)$$

the inertial terms in the  $x$ -momentum equation are  $O(\delta)$ . The leading order contribution to the rate of strain comes from  $\dot{\gamma}_{xy}$ :

$$\dot{\gamma}_{xy} = \frac{\partial u}{\partial y} + O(\delta^2). \quad (2.49)$$

Similarly, in a yielded region the leading order deviatoric stresses in Eq. (2.40) are given by

$$\tau_{k,xy} = \left[ \mu_k + \frac{\tau_{k,Y}}{\left| \frac{\partial u}{\partial y} \right|} \right] \frac{\partial u}{\partial y} + O(\delta^2), \quad (2.50)$$

where the dimensionless viscosities  $\mu_k$  are

$$\mu_k = \frac{\hat{\mu}_k \hat{u}_*}{\hat{D}^2 \Delta \hat{\rho} \hat{g} \cos \beta}, \quad k = c, m, \quad (2.51)$$

and the dimensionless yield stresses  $\tau_{k,Y}$  are

$$\tau_{k,Y} = \frac{\hat{\tau}_{k,Y}}{\Delta \hat{\rho} \hat{g} \cos \beta \hat{D}}, \quad k = c, m. \quad (2.52)$$

An  $O(\delta^2)$  uniaxial approximation to the full constitutive laws is

$$\left| \frac{\partial u}{\partial y} \right| = 0 \Leftrightarrow |\tau_k(u)| \leq \tau_{k,Y}, \quad (2.53)$$

$$\left| \frac{\partial u}{\partial y} \right| > 0 \Rightarrow \tau_k(u) = \left[ \mu_k + \frac{\tau_{k,Y}}{\left| \frac{\partial u}{\partial y} \right|} \right] \frac{\partial u}{\partial y}, \quad (2.54)$$

where

$$\tau_k(u) \sim \tau_{k,xy}(u) + O(\delta^2),$$

and the  $xy$  subscripts are dispensed with, since there is only a single shear stress.

Neglecting terms of  $O(\delta)$  leads to the following leading order uniaxial model:

$$p = p(x, t), \quad (2.55)$$

$$\frac{1}{\phi} \left[ \frac{dp}{dx} + \phi_c \right] = \frac{\partial \tau_c}{\partial y}(u), \quad y \in [0, h(x, t)), \quad (2.56)$$

$$\frac{1}{\phi} \left[ \frac{dp}{dx} + \phi_m \right] = \frac{\partial \tau_m}{\partial y}(u), \quad y \in (h(x, t), 1], \quad (2.57)$$

$$\frac{\partial h}{\partial t} + \frac{\partial Q_c}{\partial x} = 0, \quad (2.58)$$

$$u(x, 0, t) = u(x, 1, t) = 0, \quad (2.59)$$

$$u(x, h, t) = u_{\text{int}}, \quad (2.60)$$

$$\tau_c(x, h, t) = \tau_m(x, h, t) = \tau_i(x, t), \quad (2.61)$$

where  $\tau_i(x, t)$  denotes the interfacial shear stress.

### 2.2.1. Exchange flows and physical constraints

The remainder of the paper considers solutions to Eqs. (2.55), (2.56), (2.57), (2.58), (2.59), (2.60) and (2.61) which also satisfy the no net-flow constraint:

$$Q(u) = 0. \quad (2.62)$$

Furthermore, it can be assumed that for non-trivial  $u$ , Eq. (2.62) is satisfied only with

$$Q_c(u) < 0, \quad Q_m(u) > 0. \quad (2.63)$$

This is proven rigorously in Ref. [13]. A number of physically based mathematical conditions must be satisfied by the solutions to Eqs. (2.55), (2.56), (2.57), (2.58), (2.59), (2.60) and (2.61).

(i) *Buoyancy condition*: The flow is axial and since Eq. (2.62) implies that there is no imposed flow rate, the flow can be driven only by the density difference between the fluids. Consequently, it is reasonable to suppose that the pressure gradients will be limited by the static gradient of the two fluids, which dimensionlessly means

$$\phi_m < -\frac{dp}{dx} < \phi_c. \quad (2.64)$$

(ii) *Wall stress conditions*: Denote the wall shear stresses by  $\tau_{c,w}$  and  $\tau_{m,w}$  respectively, i.e.

$$\tau_{c,w} = \tau_c(y = 0), \quad (2.65)$$

$$\tau_{m,w} = \tau_m(y = 1). \quad (2.66)$$

Suppose that  $\tau_{c,w} \geq -\tau_{c,Y}$ . The buoyancy condition Eqs. (2.64) and (2.56) implies that  $\tau_{c,w}$  increases for  $y \in (0, h)$ . Since  $\tau_{c,w} \geq -\tau_{c,Y}$ , it follows that

$$\frac{\partial u}{\partial y} \geq 0 \Leftrightarrow Q_c \geq 0,$$

which is a contradiction of Eq. (2.63).

Similarly suppose that  $\tau_{m,w} \geq -\tau_{m,Y}$ . The buoyancy condition Eqs. (2.64) and (2.57) imply that  $\tau_{m,w}$  decreases for  $y \in (h, 1)$ . Since  $\tau_{m,w} \geq -\tau_{m,Y}$ , it follows that

$$\frac{\partial u}{\partial y} \geq 0 \Rightarrow Q_m \leq 0,$$

which again contradicts Eq. (2.63).

Therefore, necessary conditions for a non-trivial exchange flow are that

$$\tau_{c,w} < -\tau_{c,Y}, \quad (2.67)$$

$$\tau_{m,w} < -\tau_{m,Y}, \quad (2.68)$$

i.e. both fluids must be yielded at their contact with the walls of the slot.

(iii) *Interface stress condition*: Suppose that conditions Eqs. (2.64), (2.67) and (2.68) are satisfied. Suppose also that there is a layer of unyielded flow within both fluids at the interface. This unyielded region moves with uniform speed  $u_{int}$ . A necessary condition for there to be this unyielded region is that  $\tau_i \leq \min\{\tau_{c,Y}, \tau_{m,Y}\}$ , i.e. because the wall shear stresses are negative and the shear stresses increase linearly within each fluid, towards the fluid–fluid interface.

Consider first the cement flow. Condition Eq. (2.67) implies there is no unyielded region at  $y = 0$ . Since also  $\tau_i \leq \min\{\tau_{c,Y}, \tau_{m,Y}\}$ ,

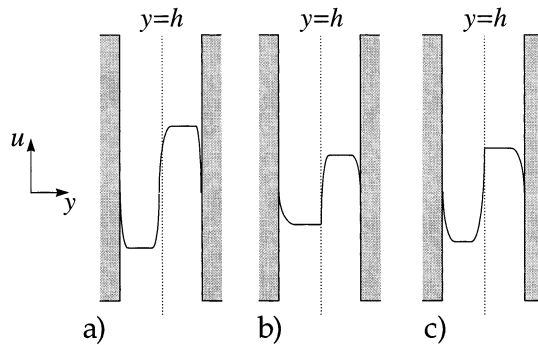


Fig. 2. Schematic of different feasible exchange flow velocity profiles: (a) Type A; (b) Type B; (c) Type C.

$$\frac{\partial u}{\partial y} \leq 0, \quad \forall y \in [0, h),$$

with strict inequality close to  $y = 0$ . Consequently,  $u_{\text{int}} < 0$ . However, Eq. (2.68) also implies there is no unyielded region at  $y = 1$  and  $\tau_i \leq \min\{\tau_{c,Y}, \tau_{m,Y}\}$  implies

$$\frac{\partial u}{\partial y} \leq 0, \quad \forall y \in (h, 1],$$

with strict inequality close to  $y = 1$ . Consequently,  $u_{\text{int}} > 0$ , which produces a contradiction. Therefore, a necessary condition for non-trivial exchange flow is that

$$\tau_i > \min\{\tau_{c,Y}, \tau_{m,Y}\}, \quad (2.69)$$

i.e. at least one fluid must have yielded at the fluid–fluid interface.

The consequence of the above conditions, Eqs. (2.64), (2.67), (2.68) and (2.69), in terms of the feasible velocity profiles for a non-zero exchange flow is illustrated schematically in Fig. 2.

### 3. Non-trivial exchange flows

The main aim of this paper is to develop qualitative understanding of the types of solution that can exist for this buoyancy driven flow. It is apparent that axial and temporal variations in Eqs. (2.55), (2.56), (2.57), (2.58), (2.59), (2.60) and (2.61) occur only in the mass conservation equation (Eq. (2.58)). A natural method of analysis is therefore to uncouple the momentum balance, compute the velocity field for given  $h$ , at each  $(x, t)$ , and then advance the interface spatially and temporally using Eq. (2.58). Under certain conditions, it will not be possible to find a non-trivial velocity solution to the momentum balance. This must be expected for any generalised Newtonian fluid with a yield stress. If the yield stress is large enough the finite (buoyancy) pressure gradient will be unable to overcome the yield stress. For example, with a single Bingham fluid in a slot driven by an axial pressure gradient, the analogous dimensionless condition for there to be only the trivial solution  $u = 0$ , to the momentum balance is:

$$\tau_Y \geq 1. \quad (3.1)$$

The aim here is to find analogous conditions on  $(\tau_{c,Y}, \tau_{m,Y})$  for which  $u = 0$  is the only solution also satisfying Eq. (2.62).

Note that the pressure gradient is unknown in Eqs. (2.56) and (2.57) and must be determined, within the bounds of Eq. (2.64), so that Eq. (2.62) is satisfied. Integrating Eqs. (2.56) and (2.57) produces:

$$\frac{h}{\phi} \left[ \frac{dp}{dx} + \phi_c \right] = \tau_i - \tau_{c,w}, \quad (3.2)$$

$$\frac{1-h}{\phi} \left[ \frac{dp}{dx} + \phi_m \right] = \tau_{m,w} - \tau_i, \quad (3.3)$$

from which

$$\frac{dp}{dx} = \phi[\tau_{m,w} - \tau_{c,w}] - [h\phi_c + (1-h)\phi_m], \quad (3.4)$$

$$\tau_i = h(1-h) + (1-h)\tau_{c,w} + h\tau_{m,w}. \quad (3.5)$$

Integrating once more produces pointwise expressions for the shear stress:

$$\tau_c(y) = y(1-h) + (1-y)\tau_{c,w} + y\tau_{m,w}, \quad y \in [0, h], \quad (3.6)$$

$$\tau_m(y) = h(1-y) + (1-y)\tau_{c,w} + y\tau_{m,w}, \quad y \in (h, 1], \quad (3.7)$$

### 3.1. Non-existence

Observe that Eqs. (3.6) and (3.7) can be straightforwardly integrated using the constitutive laws Eqs. (2.53) and (2.54) to give the velocity field in each fluid. However, although the interfacial stress is the same in both Eqs. (3.6) and (3.7), the velocity has not been matched at the interface and nor has Eq. (2.62) been satisfied. Thus, integration of Eqs. (3.6) and (3.7) gives say  $z_c(h, \tau_{c,w}, \tau_{m,w})$  and  $z_m(h, \tau_{c,w}, \tau_{m,w})$ , defined by

$$z_c(h, \tau_{c,w}, \tau_{m,w}) = \begin{bmatrix} u_{\text{int},c}(h, \tau_{c,w}, \tau_{m,w}) \\ -Q_c(h, \tau_{c,w}, \tau_{m,w}) \end{bmatrix}, \quad (3.8)$$

$$z_m(h, \tau_{c,w}, \tau_{m,w}) = \begin{bmatrix} u_{\text{int},m}(h, \tau_{c,w}, \tau_{m,w}) \\ Q_m(h, \tau_{c,w}, \tau_{m,w}) \end{bmatrix}, \quad (3.9)$$

Here  $u_{\text{int},c}(h, \tau_{c,w}, \tau_{m,w})$  is the interface velocity obtained by integrating Eq. (3.6), using the no-slip condition Eq. (2.59) at  $y=0$ , and  $u_{\text{int},m}(h, \tau_{c,w}, \tau_{m,w})$  is the interface velocity obtained by integrating Eq. (3.7), using the no-slip condition Eq. (2.59) at  $y=1$ . Define the objective functional  $Z(h, \tau_{c,w}, \tau_{m,w}) \geq 0$  by say

$$Z(h, \tau_{c,w}, \tau_{m,w}) = \|z_c - z_m\|^2, \quad (3.10)$$

( $\|\cdot\|$  denoting the Euclidean norm), and consider minimising  $Z(h, \tau_{c,w}, \tau_{m,w})$  over all feasible wall shear stresses  $(\tau_{c,w}, \tau_{m,w})$ .

In order to satisfy Eq. (2.62) and continuity of velocity at the interface,  $Z(h, \tau_{c,w}, \tau_{m,w}) = 0$  will be necessary. If this possibility can be discounted, there can be no non-zero exchange flow. Examining the constraint set for the minimisation of  $Z(h, \tau_{c,w}, \tau_{m,w})$  therefore gives a straight forward way of establishing that no non-trivial solution exists.

For fixed  $h$ , conditions Eqs. (2.64), (2.67), (2.68) and (2.69) translate into constraints on  $(\tau_{c,w}, \tau_{m,w})$ . For ease of analysis, first consider the linear translation:

$$\tilde{\tau}_c = -\tau_{c,w} - \tau_{c,Y}, \quad (3.11)$$

$$\tilde{\tau}_m = -\tau_{m,w} - \tau_{m,Y}. \quad (3.12)$$

Clearly,  $Z(h, \tau_{c,w}, \tau_{m,w})$  can be trivially redefined in terms of  $(\tilde{\tau}_c, \tilde{\tau}_m)$ , and is denoted  $Z(h, \tilde{\tau}_c, \tilde{\tau}_m)$ . The constraints Eqs. (2.64), (2.67), (2.68) and (2.69) become

$$\tilde{\tau}_m - \tilde{\tau}_c < 1 - h + \tau_{c,Y} - \tau_{m,Y}, \quad (3.13)$$

$$\tilde{\tau}_c - \tilde{\tau}_m < h + \tau_{m,Y} - \tau_{c,Y}, \quad (3.14)$$

$$\tilde{\tau}_c > 0, \quad (3.15)$$

$$\tilde{\tau}_m > 0, \quad (3.16)$$

$$h\tilde{\tau}_m + (1-h)\tilde{\tau}_c < F(h, \tau_{c,Y}, \tau_{m,Y}), \quad (3.17)$$

where

$$F(h, \tau_{c,Y}, \tau_{m,Y}) \equiv h(1-h) - (1-h)\tau_{c,Y} - h\tau_{m,Y} - \min\{\tau_{c,Y}, \tau_{m,Y}\}. \quad (3.18)$$

The constrained set of feasible  $(\tilde{\tau}_c, \tilde{\tau}_m)$  is denoted  $\Phi$  and is visualised in the  $(\tilde{\tau}_c, \tilde{\tau}_m)$  plane as a triangular region of the positive quadrant, see Fig. 3. Solution of the momentum balance, in terms of  $(\tilde{\tau}_c, \tilde{\tau}_m)$  is equivalent to

$$\{(\tilde{\tau}_c, \tilde{\tau}_m) \in \Phi : Z(h, \tilde{\tau}_c, \tilde{\tau}_m) = 0\}, \quad (3.19)$$

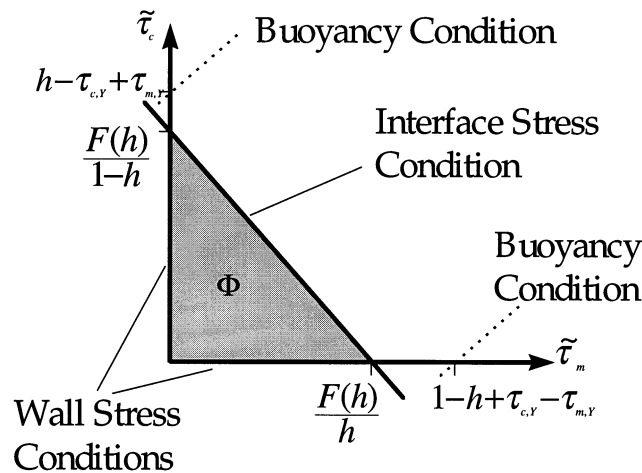


Fig. 3. Schematic of the set  $\Phi$  in the  $(\tilde{\tau}_c, \tilde{\tau}_m)$  plane, showing the different flow constraints.

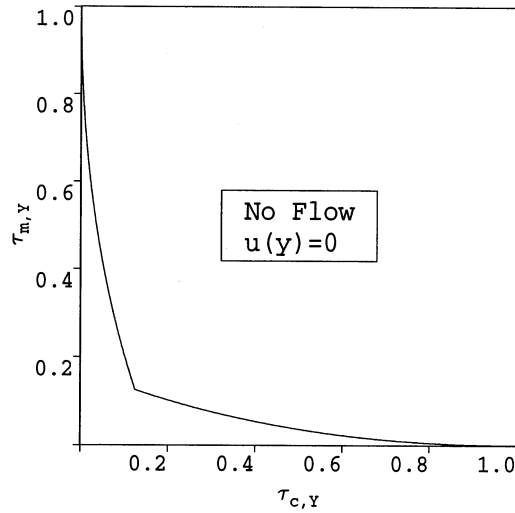


Fig. 4. Curve in the  $(\tau_{c,Y}, \tau_{m,Y})$  plane, above which no non-zero exchange flows can exist.

which could be solved with a standard constrained minimisation algorithm, (but see comments in Section 4).

From Fig. 3 it is clear that there can only be a solution to the momentum balance provided that  $F(h, \tau_{c,Y}, \tau_{m,Y}) > 0$  for at least some values of  $(h, \tau_{c,Y}, \tau_{m,Y})$ . For given fluid yield stresses, a sufficient condition for there not to exist a non-trivial exchange flow is therefore

$$F(h, \tau_{c,Y}, \tau_{m,Y}) < 0, \quad \forall h \in [0, 1]. \quad (3.20)$$

Note that  $F(h, \tau_{c,Y}, \tau_{m,Y})$  has a single maximum, say  $F(h^*, \tau_{c,Y}, \tau_{m,Y})$ :

$$h^* = \frac{1}{2}[1 + \tau_{c,Y} - \tau_{m,Y}], \quad (3.21)$$

$$F(h^*, \tau_{c,Y}, \tau_{m,Y}) = \frac{1}{4}[1 + (\tau_{c,Y} - \tau_{m,Y})^2 - 2(\tau_{c,Y} + \tau_{m,Y} + 2 \min\{\tau_{c,Y}, \tau_{m,Y}\})]. \quad (3.22)$$

Consequently, to ensure that no non-trivial flow exists, a sufficient condition is that

$$1 + (\tau_{c,Y} - \tau_{m,Y})^2 - 2(\tau_{c,Y} + \tau_{m,Y} + 2 \min\{\tau_{c,Y}, \tau_{m,Y}\}) < 0. \quad (3.23)$$

The non-existence curve in the  $(\tau_{c,Y}, \tau_{m,Y})$  plane is described by

$$1 + (\tau_{c,Y} - \tau_{m,Y})^2 - 2(\tau_{c,Y} + \tau_{m,Y} + 2 \min\{\tau_{c,Y}, \tau_{m,Y}\}) = 0, \quad (3.24)$$

and is plotted in Fig. 4. Physically, only positive values of  $(\tau_{c,Y}, \tau_{m,Y})$  are of interest. Furthermore, attention can be restricted to

$$|\tau_{c,Y} - \tau_{m,Y}| < 1. \quad (3.25)$$

To see this, write

$$F(h, \tau_{c,Y}, \tau_{m,Y}) = -(h - h_c)(h - h_m),$$

where  $\text{Re}(h_c) < \text{Re}(h_m)$ . If the roots  $h_c$  and  $h_m$  are complex, then  $F(h, \tau_{c,Y}, \tau_{m,Y}) < 0, \forall h \in [0, 1]$ , and there is no non-zero exchange flow. Suppose therefore, that  $h_c$  and  $h_m$  are real. Then because

$$(1 - h_c)(1 - h_m) = \tau_{m,Y} + \min\{\tau_{c,Y}, \tau_{m,Y}\} > 0, \quad (3.26)$$

$$h_c h_m = \tau_{c,Y} + \min\{\tau_{c,Y}, \tau_{m,Y}\} > 0, \quad (3.27)$$

only two cases are possible:

(i)  $(h_c, h_m) \cap [0, 1] = \emptyset$ . In this case, since  $F(h, \tau_{c,Y}, \tau_{m,Y})$  has a single maximum, it follows that  $F(h, \tau_{c,Y}, \tau_{m,Y}) < 0, \forall h \in [0, 1]$ , and hence no non-zero exchange flow can exist.

(ii)  $(h_c, h_m) \subset [0, 1]$ . Suppose that  $|\tau_{c,Y} - \tau_{m,Y}| \geq 1$ , then since  $h_c + h_m = 1 + \tau_{c,Y} - \tau_{m,Y}$ , either  $h_c + h_m \geq 2$  or  $h_c + h_m \leq 0$ , both of which are a contradiction. Consequently, Eq. (3.25) holds.

Fig. 4 provides sufficient conditions on the dimensionless yield stresses for which no non-zero exchange flow can exist. To further understand the significance of  $(h_c, h_m)$ , suppose that for a given pair  $(\tau_{c,Y}, \tau_{m,Y})$ , satisfying Eq. (3.25),

$$1 + (\tau_{c,Y} - \tau_{m,Y})^2 - 2(\tau_{c,Y} + \tau_{m,Y} + 2 \min\{\tau_{c,Y}, \tau_{m,Y}\}) > 0. \quad (3.28)$$

In this case there exist real  $(h_c, h_m) \subset [0, 1]$  such that  $F(h, \tau_{c,Y}, \tau_{m,Y}) > 0, \forall h \in (h_c, h_m)$ . If for  $h \in (h_c, h_m)$ , a non-zero exchange flow exists, then the behaviour as  $h \rightarrow h_c$  or as  $h \rightarrow h_m$  is easily understood by reference to Fig. 3. In either of these limits, the triangular region representing the constraint set  $\Phi$  vanishes smoothly to  $\emptyset$ . Both the wall shear stress and interface stress conditions will be satisfied identically for both fluids in this limit:

$$\tau_{c,w} \rightarrow \tau_{c,Y}, \quad (3.29)$$

$$\tau_{m,w} \rightarrow \tau_{m,Y}, \quad (3.30)$$

$$\tau_i \rightarrow \min\{\tau_{c,Y}, \tau_{m,Y}\}. \quad (3.31)$$

Since the shear stresses vary linearly across the fluid layers, the yield stresses are nowhere exceeded and the fluid velocity is identically zero in both fluid layers.

### 3.2. Existence

The only parameter space where a non-zero solution to the slot exchange flow problem can exist is for  $h \in (h_c, h_m)$  and when the yield stresses  $(\tau_{c,Y}, \tau_{m,Y})$  lie beneath the no-flow curve Eq. (3.24) in Fig. 4. In this situation, the set  $\Phi$  is non-empty, but there is still no guarantee that a non-trivial solution can be found. Since  $\Phi$  vanishes in the limits  $h \rightarrow h_c$  and  $h \rightarrow h_m$ , it is sensible to consider the question of existence close to these limits. This allows a perturbation method to be used which, although not general for all  $h \in (h_c, h_m)$ , is at least constructive.

Note that generally  $\tau_{c,Y} \neq \tau_{m,Y}$ , so that typically if  $h$  is sufficiently close to either  $h_c$  or  $h_m$ , (implying  $\tau_i \sim \min\{\tau_{c,Y}, \tau_{m,Y}\}$ ), only one of the fluids will be yielded at the interface. Thus, a solution of either type B or C will exist, see Fig. 2. Additionally, for  $\tau_{c,Y} \neq \tau_{m,Y}$  and sufficiently close to the no-flow curve of Fig. 4, the solution will be of either type B or C, for all  $h \in (h_c, h_m)$ . Fig. 5 shows those areas of the  $(\tau_{c,Y}, \tau_{m,Y})$  plane in which only solutions of type B or C will exist. These regions are bounded by Eq. (3.24) and the curve

$$1 + (\tau_{c,Y} - \tau_{m,Y})^2 - 2(\tau_{c,Y} + \tau_{m,Y} + 2 \max\{\tau_{c,Y}, \tau_{m,Y}\}) = 0. \quad (3.32)$$

Outside of this region for  $\tau_{c,Y} \neq \tau_{m,Y}$ , solutions of type A can exist for  $h \in (h_{c,A}, h_{m,A}) \subset (h_c, h_m)$ . Here  $h_{c,A}$  and  $h_{m,A}$  are the solutions of

$$0 = h(1 - h) - (1 - h)\tau_{c,Y} - h\tau_{m,Y} - \max\{\tau_{c,Y}, \tau_{m,Y}\}. \tag{3.33}$$

The case  $\tau_{c,Y} = \tau_{m,Y}$  is of mathematical interest, but is insignificant practically speaking.

In order to examine existence of  $u \neq 0$ , the perturbation method is applied both close to the no-flow curve of Fig. 4 and far from this curve, (see Section 3.2.2).

### 3.2.1. Far from the no-flow curve

Consider the following four interface perturbations, for  $\epsilon \ll 1$ :

1. Case 1: Type C solution;  $\tau_{c,Y} < \tau_{m,Y}$ ,  $h = h_c + \epsilon$ .
2. Case 2: Type C solution;  $\tau_{c,Y} < \tau_{m,Y}$ ,  $h = h_m - \epsilon$ .
3. Case 3: Type B solution;  $\tau_{c,Y} > \tau_{m,Y}$ ,  $h = h_c + \epsilon$ .
4. Case 4: Type B solution;  $\tau_{c,Y} > \tau_{m,Y}$ ,  $h = h_m - \epsilon$ .

The result of the interface perturbation is to perturb  $F(h, \tau_{c,Y}, \tau_{m,Y})$  to

$$F(h, \tau_{c,Y}, \tau_{m,Y}) = \epsilon(h_m - h_c) - \epsilon^2. \tag{3.34}$$

from which it follows that  $(\tilde{\tau}_c, \tilde{\tau}_m)$  are  $O(\epsilon)$ , provided that

$$\epsilon \ll h_m - h_c. \tag{3.35}$$

which effectively bounds the analysis away from the vicinity of the no-flow curve Eq. (3.24). The case  $h_m - h_c \sim \epsilon$  is considered in detail in Section 3.2.2. The interface shear stress is perturbed to

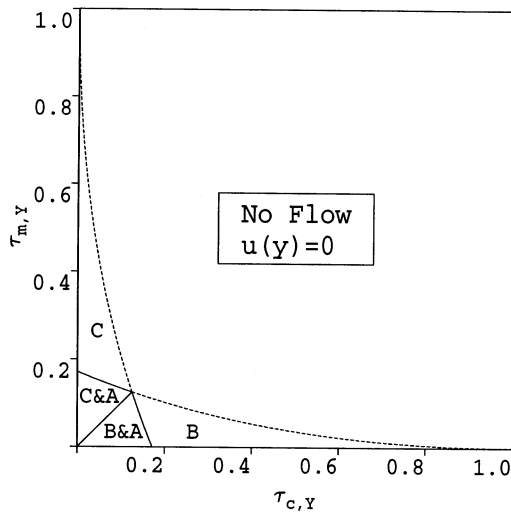


Fig. 5. Regions in the  $(\tau_{c,Y}, \tau_{m,Y})$  plane, in which only type B or type C exchange flows can exist.

$$\tau_i = \begin{cases} -[h_c \tilde{\tau}_m + (1 - h_c) \tilde{\tau}_c] - \epsilon[\tilde{\tau}_m - \tilde{\tau}_c] + F(h, \tau_{c,Y}, \tau_{m,Y}) + \min\{\tau_{c,Y}, \tau_{m,Y}\}, & \text{Cases 1 and 3,} \\ -[h_m \tilde{\tau}_m + (1 - h_m) \tilde{\tau}_c] + \epsilon[\tilde{\tau}_m - \tilde{\tau}_c] + F(h, \tau_{c,Y}, \tau_{m,Y}) + \min\{\tau_{c,Y}, \tau_{m,Y}\}, & \text{Cases 2 and 4.} \end{cases} \quad (3.36)$$

Since,  $F(h_c, \tau_{c,Y}, \tau_{m,Y}) = F(h_m, \tau_{c,Y}, \tau_{m,Y}) = 0$ , (by definition), and  $F$  is a smooth function, it is clear that by taking  $\epsilon$  sufficiently small one can ensure that

$$\min\{\tau_{c,Y}, \tau_{m,Y}\} < \tau_i < \max\{\tau_{c,Y}, \tau_{m,Y}\}, \quad (3.37)$$

so that the solution can only be of type B or C, as stated. To leading order, the condition Eq. (3.17) is

$$\epsilon[h_m - h_c] > \begin{cases} h_c \tilde{\tau}_m + (1 - h_c) \tilde{\tau}_c, & \text{Cases 1 and 3,} \\ h_m \tilde{\tau}_m + (1 - h_m) \tilde{\tau}_c, & \text{Cases 2 and 4,} \end{cases} \quad (3.38)$$

so that to leading order in  $\epsilon$ ,  $(\tilde{\tau}_c, \tilde{\tau}_m) \in \Phi$  are positive and satisfy Eq. (3.38). The shear stresses in the cement and mud are

$$\tau_c(y) = \begin{cases} y(h_m + \tilde{\tau}_c - \tilde{\tau}_m - \epsilon) - \tau_{c,Y} - \tilde{\tau}_c, & \text{Cases 1 and 3,} \\ y(h_c + \tilde{\tau}_c - \tilde{\tau}_m + \epsilon) - \tau_{c,Y} - \tilde{\tau}_c, & \text{Cases 2 and 4,} \end{cases} \quad (3.39)$$

$$\tau_m(y) = \begin{cases} (1 - y)(1 - h_m - \tilde{\tau}_c + \tilde{\tau}_m + \epsilon) - \tau_{m,Y} - \tilde{\tau}_m, & \text{Cases 1 and 3} \\ (1 - y)(1 - h_c - \tilde{\tau}_c + \tilde{\tau}_m - \epsilon) - \tau_{m,Y} - \tilde{\tau}_m, & \text{Cases 2 and 4.} \end{cases} \quad (3.40)$$

Taking  $\epsilon$  sufficiently small, there are three yield surfaces across the slot width, denoted  $y_{Y,1}$ ,  $y_{Y,2}$ ,  $y_{Y,3}$ , where  $y_{Y,1} \leq y_{Y,2} \leq y_{Y,3}$ . These are given by

$$y_{Y,1} = \begin{cases} \frac{\tilde{\tau}_c}{h_m} + O(\epsilon^2), & \text{Cases 1 and 3,} \\ \frac{\tilde{\tau}_c}{h_c} + O(\epsilon^2), & \text{Cases 2 and 4,} \end{cases} \quad (3.41)$$

$$y_{Y,2} = \begin{cases} h_c + \epsilon - \frac{\epsilon(h_m - h_c) - (1 - h_c)\tilde{\tau}_c - h_c \tilde{\tau}_m}{h_m} + O(\epsilon^2), & \text{Case 1,} \\ h_m - \epsilon - \frac{\epsilon(h_m - h_c) - (1 - h_m)\tilde{\tau}_c - h_m \tilde{\tau}_m}{h_c} + O(\epsilon^2), & \text{Case 2,} \\ h_c + \epsilon + \frac{\epsilon(h_m - h_c) - (1 - h_c)\tilde{\tau}_c - h_c \tilde{\tau}_m}{1 - h_m} + O(\epsilon^2), & \text{Case 3} \\ h_m - \epsilon + \frac{\epsilon(h_m - h_c) - (1 - h_m)\tilde{\tau}_c - h_m \tilde{\tau}_m}{1 - h_c} + O(\epsilon^2), & \text{Case 4,} \end{cases} \quad (3.42)$$

$$1 - y_{Y,3} = \begin{cases} \frac{\tilde{\tau}_m}{1 - h_m} + O(\epsilon^2), & \text{Cases 1 and 3,} \\ \frac{\tilde{\tau}_m}{1 - h_c} + O(\epsilon^2), & \text{Cases 2 and 4.} \end{cases} \quad (3.43)$$

At leading order, interface velocities and area flow rates are

$$u_{\text{int},c} = \begin{cases} \frac{-\tilde{\tau}_c^2 + (\epsilon[h_m - h_c] - \tilde{\tau}_c[1 - h_c] - \tilde{\tau}_m h_c)^2}{2h_m \mu_c} + O(\epsilon^3), & \text{Case 1,} \\ \frac{-\tilde{\tau}_c^2 + (\epsilon[h_m - h_c] - \tilde{\tau}_c[1 - h_m] - \tilde{\tau}_m h_m)^2}{2h_c \mu_c} + O(\epsilon^3), & \text{Case 2,} \\ -\frac{\tilde{\tau}_c^2}{2h_m \mu_c} + O(\epsilon^3), & \text{Case 3,} \\ -\frac{\tilde{\tau}_c^2}{2h_c \mu_c} + O(\epsilon^3), & \text{Case 4,} \end{cases} \quad (3.44)$$

$$u_{\text{int},m} = \begin{cases} \frac{\tilde{\tau}_m^2}{2(1 - h_m)\mu_m} + O(\epsilon^3), & \text{Case 1,} \\ \frac{\tilde{\tau}_m^2}{2(1 - h_c)\mu_m} + O(\epsilon^3), & \text{Case 2,} \\ \frac{\tilde{\tau}_m^2 - (\epsilon[h_m - h_c] - \tilde{\tau}_c[1 - h_c] - \tilde{\tau}_m h_c)^2}{2(1 - h_m)\mu_m} + O(\epsilon^3), & \text{Case 3,} \\ \frac{\tilde{\tau}_m^2 - (\epsilon[h_m - h_c] - \tilde{\tau}_c[1 - h_m] - \tilde{\tau}_m h_m)^2}{2(1 - h_c)\mu_m} + O(\epsilon^3), & \text{Case 4,} \end{cases} \quad (3.45)$$

$$Q_c = \begin{cases} -\frac{\tilde{\tau}_c^2 h_c}{2h_m \mu_c} + O(\epsilon^3), & \text{Cases 1 and 3,} \\ -\frac{\tilde{\tau}_c^2 h_m}{2h_c \mu_c} + O(\epsilon^3), & \text{Cases 2 and 4,} \end{cases} \quad (3.46)$$

$$Q_m = \begin{cases} \frac{\tilde{\tau}_m^2(1 - h_c)}{2(1 - h_m)\mu_m} + O(\epsilon^3), & \text{Cases 1 and 3,} \\ \frac{\tilde{\tau}_m^2(1 - h_m)}{2(1 - h_c)\mu_m} + O(\epsilon^3), & \text{Cases 2 and 4,} \end{cases} \quad (3.47)$$

Neglecting the highest order terms in  $\epsilon$ , satisfying the no net-flow condition Eq. (2.62) and the positivity of  $(\tilde{\tau}_c, \tilde{\tau}_m)$  means that

$$\tilde{\tau}_c = \begin{cases} \kappa_c \tilde{\tau}_m, & \text{Cases 1 and 3,} \\ \kappa_m \tilde{\tau}_m, & \text{Cases 2 and 4,} \end{cases} \quad (3.48)$$

where

$$\kappa_c^2 = \frac{(1 - h_c)h_m\mu_c}{(1 - h_m)h_c\mu_m}, \quad (3.49)$$

$$\kappa_m^2 = \frac{(1 - h_m)h_c\mu_c}{(1 - h_c)h_m\mu_m}. \quad (3.50)$$

Continuity of the interface velocity implies

$$\tilde{\tau}_c \sim \begin{cases} \frac{\epsilon[h_m - h_c]}{1 - h_c + h_c/\kappa_c + (1 - h_c)^{-0.5}}, & \text{Case 1,} \\ \frac{\epsilon[h_m - h_c]}{1 - h_m + h_m/\kappa_m + (1 - h_m)^{-0.5}}, & \text{Case 2,} \\ \frac{\epsilon[h_m - h_c]}{1 - h_c + h_c/\kappa_c + h_c^{-0.5}/\kappa_c}, & \text{Case 3,} \\ \frac{\epsilon[h_m - h_c]}{1 - h_m + h_m/\kappa_m + h_m^{-0.5}/\kappa_m}, & \text{Case 4,} \end{cases} \quad (3.51)$$

giving finally

$$u_{\text{int}} \sim \begin{cases} \frac{h_c}{2(1 - h_c)h_m\mu_c} \left[ \frac{\epsilon[h_m - h_c]}{1 - h_c + h_c/\kappa_c + (1 - h_c)^{-0.5}} \right]^2, & \text{Case 1,} \\ \frac{h_m}{2(1 - h_m)h_c\mu_c} \left[ \frac{\epsilon[h_m - h_c]}{1 - h_m + h_m/\kappa_m + (1 - h_m)^{-0.5}} \right]^2, & \text{Case 2,} \\ -\frac{1}{2h_m\mu_c} \left[ \frac{\epsilon[h_m - h_c]}{1 - h_c + h_c/\kappa_c + h_c^{-0.5}/\kappa_c} \right]^2, & \text{Case 3,} \\ -\frac{1}{2h_c\mu_c} \left[ \frac{\epsilon[h_m - h_c]}{1 - h_m + h_m/\kappa_m + h_m^{-0.5}/\kappa_m} \right]^2, & \text{Case 4,} \end{cases} \quad (3.52)$$

and

$$Q_c \sim \begin{cases} -\frac{h_c}{2h_m\mu_c} \left[ \frac{\epsilon[h_m - h_c]}{1 - h_c + h_c/\kappa_c + (1 - h_c)^{-0.5}} \right]^2, & \text{Case 1,} \\ -\frac{h_m}{2h_c\mu_c} \left[ \frac{\epsilon[h_m - h_c]}{1 - h_m + h_m/\kappa_m + (1 - h_m)^{-0.5}} \right]^2, & \text{Case 2,} \\ -\frac{h_c}{2h_m\mu_c} \left[ \frac{\epsilon[h_m - h_c]}{1 - h_c + h_c/\kappa_c + h_c^{-0.5}/\kappa_c} \right]^2, & \text{Case 3,} \\ -\frac{h_m}{2h_c\mu_c} \left[ \frac{\epsilon[h_m - h_c]}{1 - h_m + h_m/\kappa_m + h_m^{-0.5}/\kappa_m} \right]^2, & \text{Case 4,} \end{cases} \quad (3.53)$$

It is straightforward to check that Eq. (3.38) is satisfied by each of the above solutions.

### 3.2.2. Close to the no-flow curve

A similar perturbation method to that Section 3.2.1 in may be applied here. Suppose that

$$h_m - h_c = 2\xi, \quad (3.54)$$

with  $\xi \ll 1$ . Note that

$$h_c = h^* - \xi, \quad (3.55)$$

$$h_m = h^* + \xi, \quad (3.56)$$

and define  $\lambda$  by

$$h = h^* + \xi\lambda. \quad (3.57)$$

Thus, for  $\lambda \in [-1, 1]$  and  $h \in [h_c, h_m]$ ,  $\lambda$  represents a rescaled interface height. Again only  $\tau_{m,Y} \neq \tau_{c,Y}$  is considered and  $\xi$  is assumed small enough to ensure that the solution can be only of either type B or C. The function  $F(h, \tau_{c,Y}, \tau_{m,Y})$  becomes

$$F(h, \tau_{c,Y}, \tau_{m,Y}) = \xi^2(1 - \lambda^2). \quad (3.58)$$

The interface shear stress and the leading order interface stress condition Eq. (3.17) are

$$\tau_i = -[(h^* + \xi\lambda)\tilde{\tau}_m + (1 - h^* - \xi\lambda)\tilde{\tau}_c] + \xi^2(1 - \lambda^2) + \min\{\tau_{c,Y}, \tau_{m,Y}\}, \quad (3.59)$$

$$\xi^2(1 - \lambda^2) > h^*\tilde{\tau}_m + (1 - h^*)\tilde{\tau}_c, \quad (3.60)$$

from which it follows that  $(\tilde{\tau}_c, \tilde{\tau}_m)$  are  $O(\xi^2)$ . The shear stresses in the cement and mud are

$$\tau_c(y) = y(h^* - \xi\lambda + \tilde{\tau}_c - \tilde{\tau}_m) - \tau_{c,Y} - \tau_c, \quad (3.61)$$

$$\tau_m(y) = (1 - y)(1 - h^* + \xi\lambda - \tilde{\tau}_c + \tilde{\tau}_m) - \tau_{m,Y} - \tau_m. \quad (3.62)$$

Again there will be three yield surfaces,  $y_{Y,1}, y_{Y,2}, y_{Y,3}$ , where  $y_{Y,1} \leq y_{Y,2} \leq y_{Y,3}$ . These are given by

$$y_{Y,1} = \frac{\tilde{\tau}_c}{h^* - \xi\lambda + \tilde{\tau}_c - \tilde{\tau}_m}, \quad (3.63)$$

$$y_{Y,2} = \begin{cases} h^* + \xi\lambda - \frac{\xi^2(1-\lambda^2) - h^*\tilde{\tau}_m - (1-h^*)\tilde{\tau}_c}{h^*} + O(\xi^3), & \tau_{c,Y} < \tau_{m,Y}, \\ h^* + \xi\lambda + \frac{\xi^2(1-\lambda^2) - h^*\tilde{\tau}_m - (1-h^*)\tilde{\tau}_c}{h^*} + O(\xi^3), & \tau_{c,Y} > \tau_{m,Y}, \end{cases} \quad (3.64)$$

$$y_{Y,3} = 1 - \frac{\tilde{\tau}_m}{1 - h^* + \xi\lambda - \tilde{\tau}_c + \tilde{\tau}_m}. \quad (3.65)$$

Interface velocities and area flow rates are

$$u_{\text{int},c} = \begin{cases} -\frac{\tilde{\tau}_c^2 + (\xi^2(1-\lambda^2) - h^*\tilde{\tau}_m - (1-h^*)\tilde{\tau}_c)^2}{2h^*\mu_c} + O(\xi^5), & \tau_{c,Y} < \tau_{m,Y}, \\ -\frac{\tilde{\tau}_c^2}{2h^*\mu_c} + O(\xi^5), & \tau_{c,Y} > \tau_{m,Y}, \end{cases} \quad (3.66)$$

$$u_{\text{int},m} = \begin{cases} \frac{\tilde{\tau}_m^2}{2(1-h^*)\mu_m} + O(\xi^5), & \tau_{c,Y} < \tau_{m,Y}, \\ \frac{\tilde{\tau}_m^2 - (\xi^2(1-\lambda^2) - h^*\tilde{\tau}_m - (1-h^*)\tilde{\tau}_c)^2}{2(1-h^*)\mu_m} + O(\xi^5), & \tau_{c,Y} > \tau_{m,Y} \end{cases} \quad (3.67)$$

$$Q_c = -\frac{\tilde{\tau}_c^2}{2\mu_c} + O(\xi^5), \quad (3.68)$$

$$Q_m = -\frac{\tilde{\tau}_m^2}{2\mu_m} + O(\xi^5), \quad (3.69)$$

The leading order solution is

$$\kappa\tilde{\tau}_m = \tilde{\tau}_c \sim \begin{cases} \frac{\xi^2(1-\lambda^2)}{1 - h^* + h^*/\kappa + (1-h^*)^{-0.5}}, & \tau_{c,Y} < \tau_{m,Y}, \\ \frac{\xi^2(1-\lambda^2)}{1 - h^* + h^*/\kappa + (h^*)^{-0.5}/\kappa}, & \tau_{c,Y} > \tau_{m,Y}, \end{cases} \quad (3.70)$$

where

$$\kappa^2 = \frac{\mu_c}{\mu_m}. \quad (3.71)$$

This gives

$$u_{\text{int}} \sim \begin{cases} \frac{1}{2(1-h^*)\mu_c} \left[ \frac{\xi^2(1-\lambda^2)}{1-h^*+h^*/\kappa+(1-h^*)^{-0.5}} \right]^2, & \tau_{c,Y} < \tau_{m,Y}, \\ -\frac{1}{2h^*\mu_c} \left[ \frac{\xi^2(1-\lambda^2)}{1-h^*+h^*/\kappa+(h^*)^{-0.5/\kappa}} \right]^2, & \tau_{c,Y} > \tau_{m,Y}. \end{cases} \quad (3.72)$$

$$Q_c \sim \begin{cases} -\frac{1}{2\mu_c} \left[ \frac{\xi^2(1-\lambda^2)}{1-h^*+h^*/\kappa+(1-h^*)^{-0.5}} \right]^2, & \tau_{c,Y} < \tau_{m,Y}, \\ -\frac{1}{2\mu_c} \left[ \frac{\xi^2(1-\lambda^2)}{1-h^*+h^*/\kappa+(h^*)^{-0.5/\kappa}} \right]^2, & \tau_{c,Y} > \tau_{m,Y}. \end{cases} \quad (3.73)$$

#### 4. Interface propagation

From the results of Section 3.2.2. it is now possible to make a preliminary study of interface propagation. Rescaling the dimensionless time:

$$t = \tilde{t}\omega, \quad (4.1)$$

where

$$\omega = \begin{cases} \frac{2\mu_c[1-h^*+h^*/\kappa+(1-h^*)^{-0.5}]^2}{\xi^3} & \tau_{c,Y} < \tau_{m,Y}, \\ \frac{2\mu_c[1-h^*+h^*/\kappa+(h^*)^{-0.5/\kappa}]^2}{\xi^3} & \tau_{c,Y} > \tau_{m,Y}, \end{cases} \quad (4.2)$$

and defining  $f(\lambda)$  by:

$$f(\lambda) = \begin{cases} -(1-\lambda^2)^2, & |\lambda| \leq 1, \\ 0, & |\lambda| > 1, \end{cases} \quad (4.3)$$

the perturbed interface evolution problem is:

$$\frac{\partial \lambda}{\partial \tilde{t}} + \frac{\partial}{\partial x} f(\lambda) = 0. \quad (4.4)$$

Of most interest is the long term behaviour of Eq. (4.4). The initial interface profile will propagate along the characteristics of Eq. (4.4). The characteristic velocities, say  $v_c(\lambda)$ , are given by

$$v_c(\lambda) \equiv \frac{df}{d\lambda}(\lambda) = \begin{cases} 4\lambda(1-\lambda^2), & |\lambda| \leq 1, \\ 0, & |\lambda| > 1. \end{cases} \quad (4.5)$$

Both  $f(\lambda)$  and  $v_c(\lambda)$  are plotted in Fig. 6.

The maximum characteristic speeds  $\pm v_{c,\max}$  are attained at  $\lambda = \pm 1/\sqrt{3}$ :

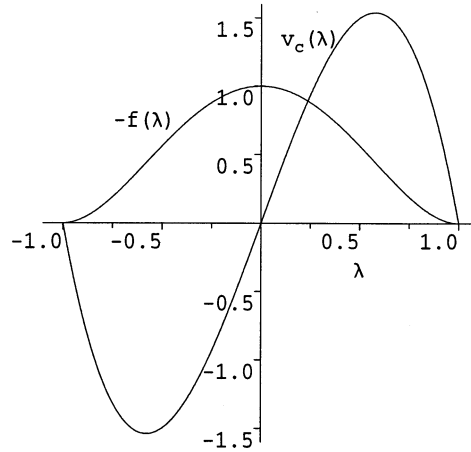


Fig. 6. Interface propagation for the re-scaled perturbation solution: flux function,  $-f(\lambda)$ , and characteristic velocity function,  $v_c(\lambda)$ .

$$v_{c,\max} = v_c\left(\frac{1}{\sqrt{3}}\right) = \frac{8}{3\sqrt{3}} \approx 1.5396, \quad (4.6)$$

for which  $f = -\frac{4}{9}$ . For  $\lambda \in [-1, -1/\sqrt{3})$  and for  $\lambda \in (1/\sqrt{3}, 1]$ , front-steepening is expected to occur, (i.e. a shock-like phenomena). Eventually, the interface profile will advance up and down the slot at the two heights  $\lambda = \pm 1/\sqrt{3}$  with speeds  $\pm v_{c,\max}$ , respectively. For  $\lambda \in (-1/\sqrt{3}, 1/\sqrt{3})$  the interface is *stretched out*, as shown schematically in Fig. 7. This behaviour will be relatively independent of the initial conditions.

In dimensional terms, the maximum characteristic speed computed from the perturbation solution, say  $\hat{v}_{c,\max}$ , is given by

$$\hat{v}_{c,\max} = \frac{\hat{D}^2 \Delta \hat{\rho} \hat{g} \cos \beta}{[\hat{\mu}_c \hat{\mu}_m]^{1/2}} v(\tau_{c,Y}, \tau_{m,Y}, \kappa), \quad (4.7)$$

where

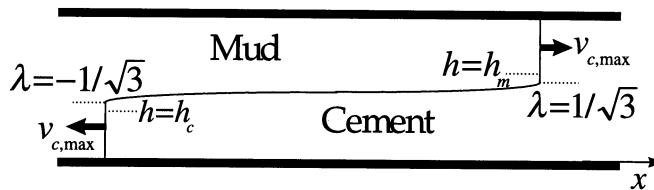


Fig. 7. Schematic of the interface propagation behaviour at long times for the rescaled perturbation solution.

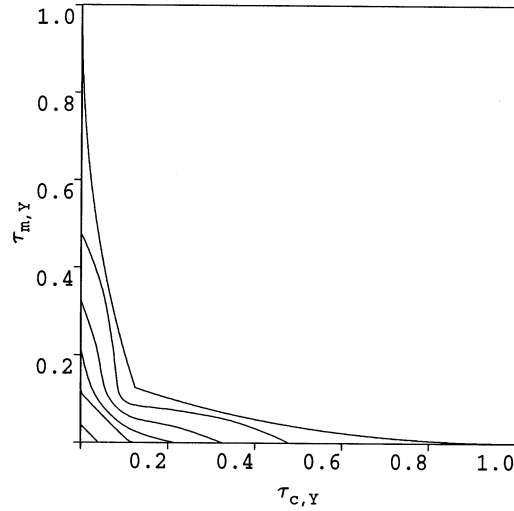


Fig. 8. Contour plot for the function  $v(\tau_{c,Y}, \tau_{m,Y}, 1)$ ; contours plotted at intervals  $\Delta v = 0.003$ , note  $v(0, 0, 1) \approx 0.0165$ .

$$v(\tau_{c,Y}, \tau_{m,Y}, \kappa) = \begin{cases} \frac{4\xi^3}{3\sqrt{3\kappa}[1 - h^* + h^*/\kappa + (1 - h^*)^{-0.5}]^2} & \tau_{c,Y} < \tau_{m,Y}, \\ \frac{4\xi^3}{3\sqrt{3\kappa}[1 - h^* + h^*/\kappa + (h^*)^{-0.5}/\kappa]^2} & \tau_{c,Y} > \tau_{m,Y}. \end{cases} \quad (4.8)$$

Note that

$$\xi = \sqrt{F(h^*, \tau_{c,Y}, \tau_{m,Y})}, \quad (4.9)$$

with  $F(h^*, \tau_{c,Y}, \tau_{m,Y})$  and  $h^*(\tau_{c,Y}, \tau_{m,Y})$  defined by Eqs. (3.21) and (3.22), respectively. The function  $v(\tau_{c,Y}, \tau_{m,Y}, \kappa)$  is plotted in Fig. 8 for  $\kappa = 1$ . Note that  $v(\tau_{c,Y}, \tau_{m,Y}, \kappa) = 0$  on the no-flow curve Eq. (3.24).

#### 4.1. Computational solution of the full problem

Strictly speaking, the perturbation solution treated above becomes invalid sufficiently far away from the no-flow curve Eq. (3.24), as the parameter  $\xi$  increases. Fig. 9 shows the variation of  $\xi$  in this range. Clearly  $\xi \ll 1$  is a fairly small envelope close to Eq. (3.24). It is questionable whether the perturbation solution is useful outside this range or whether computational solution of the full problem is necessary.

Certainly, computational solution of the full problem is quite possible, for example via the formulation described in Section 3.1. This constitutes a constrained optimisation problem in the two variables  $(\hat{\tau}_c, \hat{\tau}_m)$ . The objective functional is smooth and with a little algebraic effort, (semi-)analytic expressions for both  $z_c$  and  $z_m$  can be derived. Computational solution should be relatively quick, (using e.g. a standard library subroutine), and one has the perturbation solutions of Sections 3.2.1 and 3.2.2 to use as initial guesses for the optimisation and for test solutions, respectively.

However, it is doubtful whether computational solution of the full problem really brings any additional insight. Note first of all, that the perturbation solutions of Section 3.2.2. are accurate to order  $\xi^4$ ; the error is  $O(\xi)$  times the terms in these expressions and there is nothing in the derivation to suggest that this perturbation procedure is not completely regular. Even far away from the curve (Eq. (3.24)) the flow will consist of two stratified fluid layers, each consisting of yielded and unyielded layers. The velocity magnitude is essentially determined by the dimensionless modified pressure gradients and viscosities, together with the thicknesses of the yielded fluid layers. These physical constraints are embodied in the perturbation solution and there are no additional physical phenomena to be considered. Therefore, one can expect that the orders of magnitude (at least) of the perturbation solution derived in Section 3.2.2 will remain valid outside the strict range  $\xi \ll 1$ , although quantitatively the error will become  $O(\xi)$  times the largest terms. Secondly, note that the interface propagation phenomena for the full computational solution is likely to be qualitatively very similar to that for the perturbation solution considered above. This is true if the flux  $Q_c(h)$  for  $h \in (h_c, h_m)$  is qualitatively the same as  $f(\lambda)$  for  $\lambda \in (-1, 1)$ . Note that the shear stresses (Eqs. (3.6) and (3.7)) are bilinear in  $(y, h)$  and when integrated twice should result in a quartic dependence of  $Q_c(h)$  on  $h$ , (cf.  $f(\lambda)$ ). Additionally, the perturbation solutions in Section 3.2.1 show that close to  $h_c$  and  $h_m$  the flux  $Q_c(h) \rightarrow 0$  quadratically, (cf.  $f(\lambda)$  as  $|\lambda| \rightarrow 1$ ). Finally, from Fig. 3 one sees that the constraint set for feasible  $(\hat{\tau}_c, \hat{\tau}_m)$  is largest when  $F$  attains its maximum, at  $h^*$  the midpoint of  $(h_c, h_m)$ . This suggests that larger values of  $(\hat{\tau}_c, \hat{\tau}_m)$  may satisfy Eq. (2.62) in the interior of the interval  $(h_c, h_m)$ , resulting in larger  $Q_c(h)$ . Thus, in total there is good reason to believe that the solution to the full problem is qualitatively similar to the perturbation solution already examined. This can be exhaustively verified by computation. Since the slot model has been considered mostly to provide insight into more geometrically complicated flows, there is no reason to compute an exact quantitative answer.

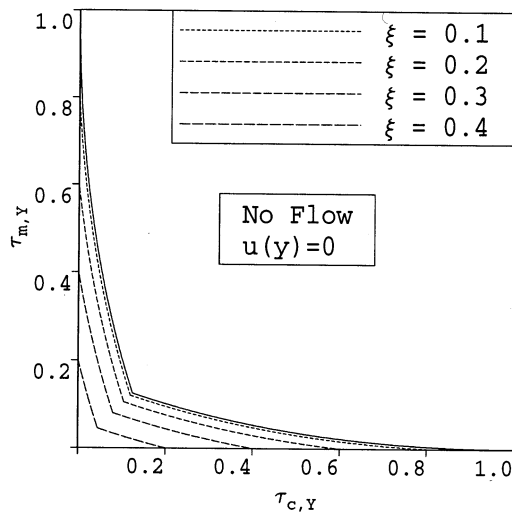


Fig. 9. Curves corresponding to different values of the perturbation parameter  $\xi$ .

## 5. Discussion

Before drawing any conclusions from the analysis developed here, it is necessary to reconsider the physical validity of the model assumptions. In the first place, when considering interface propagation it should be noted that the scaling assumptions break down close to the propagating fronts in Fig. 7, even though the interface is stretched longitudinally between the fronts. The front steepening is a physical feature of the long-thin stratified exchange flow model, but whether it occurs in reality is not proven. If this type of steepening occurs, the fluid velocity close to the advancing fronts will probably be truly multi-dimensional, since it is necessary for the fluids to displace one another.

Consider also the validity of the non-inertial assumption (Eq. (2.48)) close to the no-flow curve of Fig. 4. The dimensionless viscosities can be interpreted as Stoke's numbers for the two fluids, which compare the relative magnitudes of viscous and buoyancy forces, over the width of the channel. The velocity scale  $\hat{u}_*$  which renders the dimensionless viscosities of order unity is that for which viscous and buoyancy forces approximately balance. This velocity scale is typically very large and is indicative of the fact that typically viscous forces alone do not balance buoyancy forces in such flows, i.e.  $\mu_k \ll 1$  typically. However, slow slumping can be observed experimentally [4]. This fact is explained by the interaction between viscous and plastic forces. From Fig. 4 it is clear that typically a combination like  $\tau_{m,Y} \lesssim 1$  and  $\tau_{c,Y} \lesssim 0.1$  or  $\tau_{c,Y} \lesssim 1$  and  $\tau_{m,Y} \lesssim 0.1$  will be necessary for there to exist a non-trivial flow. The flow will be characterised by thin yielded and unyielded layers. The viscous forces come into play only in the yielded shear layers. Close to the curve in Fig. 4, these layers are of size  $\sim \xi^2$ . Typically,  $\tilde{\mu}_m \sim \tilde{\mu}_c$ , so that one can assume  $\kappa \sim 1$  for many muds and cements used. Assume that the interface velocity is indicative of the axial velocities. The velocity scale then remains valid if  $u_{\text{int}} \sim 1$ , which implies that

$$\frac{\hat{\mu}_k \hat{u}_*}{\hat{D}^2 \Delta \hat{\rho} \hat{g} \cos \beta} = \mu_k \sim \xi^4, \quad (5.1)$$

at points close below the curve in Fig. 4, but away from the axes. Combining Eq. (5.1) with the non-inertial assumption, Eq. (2.48) gives

$$\xi \sim \left[ \frac{\hat{\mu}_k}{\hat{D}^{3/2} [\hat{\rho}_k \Delta \hat{\rho} \hat{g} \cos \beta]^{1/2}} \right]^{1/4}. \quad (5.2)$$

This does not typically require small values of  $\xi$  to be valid. Thus, depending on Eq. (5.2) the regime of validity of the non-inertial assumption could be quite wide, certainly larger than the region of strict validity of the perturbation solution.

These arguments do not necessarily guarantee that a near uni-axial stratified flow will be observed. This will depend in part on the placement of the fluids (i.e. initial interface) and in part on their initial velocities. One might expect the uniaxial flow to be characteristic of a low energy (i.e. slow) initial condition.

If the stratified exchange flow exists, another consideration regarding its region of validity is that of flow stability at large velocities. Most likely to develop here might be shear and/or gravitational instabilities in the yielded fluid layer(s) close to the fluid–fluid interface. It is worth remarking that if the flow is of type B or C, then there is only one yielded fluid layer at the

interface, the other fluid acting essentially as a solid moving wall. This has the interesting consequence that it is somewhat uncertain whether the stability problem is really a one-fluid or a two-fluid problem! This problem has not been studied; relevant work here is Refs. [17–19].

To conclude, a number of insights are made:

(i) For simple stratified flows of this type, it appears that four different solution types are possible, depending on the interface position and the dimensionless yield stresses of the two fluids. The possibilities are: no flow; fluid 1 yields at their common interface but fluid 2 does not; fluid 2 yields at their common interface but fluid 1 does not; both fluid yield at their common interface.

(ii) When a non-trivial flow exists, it cannot exist for all interface heights. There always exist minimum layer thicknesses below which the yield stress is sufficient to prevent flow.

(iii) The exchange flow constraint Eq. (2.62) leads to a flow which is much more *stable*, in the sense that if the two fluids have identical yield stresses,  $\hat{\tau}_Y$ , then there would be no exchange flow for

$$\hat{\tau}_Y > \frac{\hat{D}\Delta\rho\hat{g}\cos\beta}{8}.$$

For an analogous constant pressure gradient axial flow, without the constraint (Eq. (2.62)), one would require

$$\hat{\tau}_Y > \hat{D}\Delta\rho\hat{g}\cos\beta.$$

(iv) Intuitively, one would expect that an exchange flow of the same fluids in a pipe of diameter  $\hat{D}$  will be more stable than that in the slot, (i.e. lower dimensionless yield stresses would be required to ensure  $u = 0$ ). Thus, the curve Eq. (3.24) should provide an upper bound for the analogous curve in a pipe.

(v) Lastly, note that the results presented here, regarding sufficient conditions on the yield stresses for there to be no-flow, i.e. curve Eq. (3.24), are equally valid for other common generalised Newtonian fluids with a yield stress, e.g. Casson, Herschel–Bulkley.

## Acknowledgements

Dr. John Ferguson is thanked for his freely communicated insights and understanding. The management of Schlumberger Dowell are thanked for their permission to publish this paper.

## References

- [1] C. Marca, Remedial cementing, in: E.B. Nelson (Ed.), Well Cementing, chap. 13, Schlumberger Educational Services, Houston, 1990.
- [2] R.M. Beirute, Flow behaviour of an Unset Cement Plug in Place, Society of Petroleum Engineers paper number, SPE 7589 (1978).
- [3] D.L. Bour, D.L. Sutton, P.G. Creel, Development of Effective Methods for Placing Competent Cement Plugs, Society of Petroleum Engineers paper number SPE 15008 (1986).

- [4] D.G. Calvert, J.F. Heathman, J.E. Griffith, Plug Cementing: Horizontal to Vertical Conditions, Society of Petroleum Engineers paper number, SPE 30514 (1995).
- [5] K. Harestad, T.P. Herigstad, A. Torsvoll, N.E. Nodland, A. Saasen, Optimization of Balanced-Plug Cementing, Society of Petroleum Engineers paper number SPE 33084 (1997).
- [6] R.C. Smith, R.M. Beirute, G.B. Holman, Improved Method of Setting Successful Whipstock Cement Plugs, Society of Petroleum Engineers paper number SPE 11415 (1983).
- [7] R. Byron-Bird, G.C. Dai, B.J. Yarusso, The rheology and flow of viscoplastic materials, *Rev. Chem. Engng.* 1 (1) (1983) 2–70.
- [8] S.D.R. Wilson, Squeezing flow of a Bingham material, *J. Non-Newtonian Fluid Mech.* 47 (1993) 211–219.
- [9] S.D.R. Wilson, A.J. Taylor, The channel entry problem for a yield stress fluid, *J. Non-Newtonian Fluid Mech.* 65 (1996) 165–176.
- [10] K.F. Liu, C.C. Mei, Slow spreading of a sheet of Bingham fluid on an inclined plane, *J. Fluid Mech.* 207 (1989) 505–529.
- [11] I.C. Walton, S.H. Bittleston, The axial flow of a Bingham plastic in a narrow eccentric annulus, *J. Fluid Mech.* 222 (1991) 39–60.
- [12] P. Szabo, O. Hassager, Flow of viscoplastic fluids in eccentric annular geometries, *J. Non-Newtonian Fluid Mech.* 45 (1992) 149–169.
- [13] I.A. Frigaard, O. Scherzer, Uniaxial exchange flows of two Bingham fluids in an inclined cylindrical duct, *IMA J. Appl. Math.*, accepted for publication.
- [14] G. Duvaut, J.L. Lions, *Inequalities in Mechanical and Physics*, vol. 219, Springer-Verlag, 1976, pp. 279–327.
- [15] R. Glowinski, J.L. Lions, R. Tremolieres, *Numerical Analysis of Variational Inequalities*, North-Holland, Amsterdam, 1981.
- [16] R. Glowinski, *Numerical Methods for Nonlinear Variational Problems*, Springer-Verlag, 1983.
- [17] I.A. Frigaard, S.D. Howison, I.J. Sobey, On the stability of Poiseuille flow of a Bingham fluid, *J. Fluid Mech.* 263 (1994) 133–150.
- [18] K.F. Liu, C.C. Mei, Roll waves on a layer of a muddy fluid flowing down a gentle slope—a Bingham model, *Phys. Fluids* 6 (1994) 2577–2590.
- [19] A. Pinarbasi, A. Liakopoulos, Stability of two-layer Poiseuille flow of Carreau–Yasuda and Bingham-like fluids, *J. Non-Newtonian Fluid Mech.* 57 (1995) 227–241.